ChemComm

COMMUNICATION

View Article Online
View Journal

Cite this: DOI: 10.1039/d6cc01514j

Received 13th March 2026,
Accepted 20th April 2026

DOI: 10.1039/d6cc01514j

rsc.li/chemcomm

Upcycling disposed sunscreen waste into supported catalysts for environmental purification

Toshiki Shimizu,[a] Fuminao Kishimoto,*[a] Yasuhiro Sakamoto,[a] Minh Thuan Pham,[a] Ryo Sasaki,[b] Rie Nakamura[b] and Kazuhiro Takanabe*[a]

We report a strategy for upcycling sunscreen waste into supported catalysts for environmental purification. Utilizing inherent ZnO nanoparticles and organic additives, Pt is photodeposited *via* UV irradiation without external reagents. This scalable process repurposes consumer waste into functional materials, advancing sustainable engineering and circular chemical practices.

Chemical upcycling of waste materials is increasingly recognized as a key strategy for advancing a circular economy and reducing environmental burden beyond conventional physical recycling.[1–3] While chemical upgrading of plastics has been intensively studied,[4–7] the chemical upcycling of everyday functional consumer products, such as cosmetics, has received little attention. Among cosmetic products, sunscreens are discarded in particularly large quantities due to rapid changes in consumer trends, frequent release of new formulations with improved performance, and regulatory restrictions on allowable chemical additives. While initiatives have been reported to reuse discarded cosmetics as craft materials such as paints,[8] approaches that upgrade their value through chemical transformation have not been explored.

Many commercial sunscreens contain approximately 5–25 wt% zinc oxide (ZnO) nanoparticles for broad-spectrum protection covering both UV-B and UV-A regions.[9] To enhance aesthetic appearance, these nanoparticles are uniformly sized at around 20 nm, coated with dimethylpolysiloxane (dimethicone, $H_3C\text{-}[Si(CH_3)_2O]_n\text{-}Si(CH_3)_3$), and exhibit exceptionally high crystallinity, corresponding to cosmetic-grade materials.[10,11] However, global zinc resources are limited, with the reserves-to-production ratio of Zn estimated to be approximately 18 years.[12] Notably, approximately 82.6% of zinc oxide engineered nanomaterials production is reportedly directed toward cosmetic applications.[13] Given the rapidly expanding demand for zinc-based materials in catalysis, batteries, desulfurization agents, and functional alloys,[12,14–16] the chemical upgrading of ZnO nanoparticles contained in discarded sunscreens represents an increasingly important and underexplored opportunity. Among these applications, the use of zinc compounds as catalysts—particularly in CO_2 reduction[17,18] and photocatalytic reactions[19–23]—aligns closely with recent directions in green chemistry.

In this study, we propose a novel chemical upcycling strategy that directly converts high-quality ZnO nanoparticles contained in discarded sunscreens into environmental purification catalysts without any separation steps. Although sunscreen formulations contain numerous organic additives and impurities, we exploit the intrinsic photocatalytic activity of ZnO. Upon dropwise addition of an aqueous metal salt solution (*e.g.*, H_2PtCl_6) to the sunscreen matrix and subsequent irradiation with ultraviolet light (~370 nm), ZnO is photoexcited and generates electron–hole pairs. The photogenerated holes oxidatively decompose organic components in the formulation, while the electrons reduce Pt ions, resulting in the selective deposition of Pt nanoparticles onto the ZnO surface. This process yields a highly viscous slurry containing Pt-supported ZnO catalysts. The slurry can be directly coated onto monolithic substrates or construction materials, enabling its practical application as an environmental purification catalyst for the degradation of hazardous pollutants.

Fig. 1(a) shows a transmission electron microscopy (TEM) image of commercially available dimethicone-modified ZnO nanoparticles manufactured for use in sunscreen products (MZY-505M, Tayca Corporation). The primary particle size of ZnO was approximately 20 nm, and a thin amorphous layer was observed on its surface, which was attributed to a surface coating derived from dimethicone. Thermogravimetric analysis (TGA) profiles of dimethicone-modified ZnO and the sunscreen product (sunscreen-1, marketed by KOSÉ Corporation) are shown in Fig. 1(b). Dimethicone-modified ZnO exhibited a weight loss of 1.4% upon heating to 600 °C in air, which is attributed to the oxidative decomposition of the

[a] *Department of Chemical System Engineering, School of Engineering, The University of Tokyo, 7-3-1 Hongo, Bunkyo-ku, Tokyo 113-8656, Japan. E-mail: kfuminao@chemsys.t.u-tokyo.ac.jp, takanabe@chemsys.t.u-tokyo.ac.jp*
[b] *KOSÉ Corporation, 48-18 Sakae-cho, Kita-ku, Tokyo 114-0005, Japan*

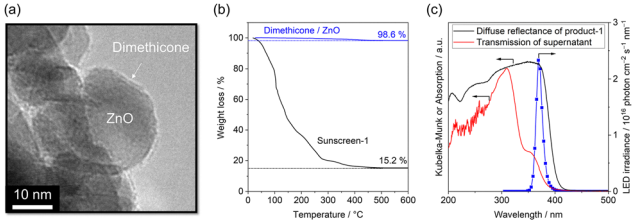

Fig. 1 (a) TEM image of dimethicone treated ZnO nanoparticles. (b) TG curve of dimethicone treated ZnO nanoparticles and the sunscreen product. Gas condition: air. (c) UV-vis spectra of the sunscreen product and its supernatant, and the photon flux of the LED light source for the photodeposition method.

dimethicone coating, with residual silicon species likely converted to SiO_2.

$$H_3C\text{-}[Si(CH_3)_2O]_n\text{-}Si(CH_3)_3 + 8(n+2)O_2 \rightarrow (n+1)SiO_2 + 2(n+2)CO_2 + 3(n+2)H_2O$$

The mass loss associated with this reaction was 18.9%. Based on the TGA results, the dimethicone content was therefore estimated to be 7.4 wt% of the total sample mass. In contrast, the sunscreen product exhibited a weight loss of 84.8% under the same conditions, leaving a residual mass of 15.2%. The formulation contains no thermally stable inorganic components other than ZnO (aside from minor amounts of silica derived from dimethicone).

The UV-vis diffuse reflectance spectrum of the sunscreen product and the transmission spectrum of the supernatant obtained after removal of the ZnO component by centrifugation and filtration are shown in Fig. 1(c). The sunscreen exhibited an absorption edge at approximately 410 nm. In contrast, the supernatant showed a markedly reduced absorption intensity in the 350–410 nm region. These results indicate that light within this wavelength range is absorbed predominantly by ZnO in the sunscreen formulation, confirming the selective photoexcitation of ZnO under near-UV irradiation. Accordingly, photodeposition onto ZnO was performed using an LED light source with a central wavelength of 370 nm (Asahi Spectra Co., Ltd; CL-1501, photon flux shown in Fig. 1(c)).

As ZnO sources, commercially available cosmetic-grade nanoparticles were used, including unmodified ZnO (MZ-500, Tayca Corporation) and dimethicone-coated ZnO. In addition, three commercially available sunscreen products (sunscreens 1–3) marketed by KOSÉ Corporation, Japan were employed in this study. The photodeposition of Pt nanoparticles under UV irradiation using these ZnO sources and their catalytic performance in CO oxidation as a demonstration reaction are summarized in Table 1. Compositional analysis by thermogravimetric (TG) measurements indicated that the ZnO content in the investigated sunscreen samples was approximately 15 wt% in all cases, with no significant differences among the products (raw profiles are shown in Fig. S1). Inductively coupled plasma (ICP) analysis of the residual inorganic components revealed that the silica content increased in the order sunscreen-1 < sunscreen-2 < sunscreen-3. Because silica is derived from the oxidative decomposition of the dimethicone coating, this trend suggests that the surface coverage of ZnO by dimethicone increases in the same order.

These sunscreens or ZnO samples (ZnO basis = 0.5 g) were dispersed in a H_2O/ethanol (EtOH) mixture and then H_2PtCl_6 aqueous solution (ZnO basis = 1 wt% Pt) was added to the dispersion. EtOH was added as a sacrificial oxidant to promote Pt photodeposition. After 12 h irradiation with a 370 nm UV-LED, the precipitates were separated by centrifugation.

Fig. S3 shows the quantitative results of H_2 evolution during light irradiation. The amount of H_2 evolved gradually increased over approximately one hour. During this period, the photoexcited electrons in ZnO are considered to have been utilized both for the reduction of Pt and for H_2 evolution, with Pt nanoparticles acting as a cocatalyst. In contrast, after sufficient irradiation time, the amount of H_2 evolution reached a constant value. This suggests that Pt reduction had been completed and that only photocatalytic H_2 evolution by Pt/ZnO subsequently proceeded.

ICP analysis of the samples obtained after UV irradiation confirmed the successful deposition of Pt onto ZnO. For unmodified ZnO, the Pt loading was nearly consistent with the initial feed amount, indicating efficient photodeposition under the applied conditions. For dimethicone-coated ZnO and sunscreen-1 and -2, the amount of deposited Pt was slightly lower than the nominal feed amount but still indicated efficient

Table 1 Composition of sunscreen creams used in this study

ZnO source	Calcination[a] residue/wt%	Silica fraction[b] (as SiO_2, ZnO basis)/wt%	Added Pt amount (ZnO basis)/wt%	Deposited[bc] Pt (ZnO basis)/wt%	CO oxidation[d] rate/mmol g_{cat}^{-1} h^{-1}
Unmodified ZnO	>99	n.t.[e]	1.0	0.97	9.6
Dimethicone treated ZnO	98.6	2.9	1.0	0.41	10.9
Sunscreen-1	15.2	4.9	1.0	0.58	7.6
Sunscreen-2	15.8	5.7	1.0	0.74	7.2
Sunscreen-3	15.1	6.7	1.0	0.03	~0
			5.0	n.t.	~0

[a] Analyzed by TG measurement up to 600 °C under air. [b] Measured by ICP-AES. [c] Photodeposition procedure: ZnO or sunscreen (ZnO basis = 0.5 g) was dispersed in 45 mL of H_2O. H_2PtCl_6 (2.64 μmol) and ethanol (30 mL) were added. UV light irradiation (370 nm) for 12 h. [d] Catalyst weight: 1.3 mg (diluted with 78.7 mg of Al_2O_3, dilution ratio = 60). Pretreatment conditions: pure H_2, 300 °C, 30 min. Reaction conditions: CO = 0.10 kPa and O_2 = 10 kPa (Ar balance), flow rate = 100 mL min^{-1} (WHSV = 4615 L g^{-1} h^{-1}), 170 °C. [e] n.t.: not tested.

photodeposition. In contrast, Pt deposition on sunscreen-3 was negligible under the same conditions.

To evaluate the catalytic performance of the obtained Pt-supported ZnO materials, CO oxidation was employed as a model reaction. CO oxidation is a prototypical reaction in automotive exhaust catalysis,[24] and Pt/ZnO systems have been extensively studied for this process.[25–30] The thermal catalytic CO oxidation reaction is a typical structure-insensitive reaction. Therefore, the size effect of Pt nanoparticles on catalytic performance is considered to be negligible. Rather, its activity reflects the number of accessible Pt surface sites under the given CO and O_2 partial pressures, providing a reliable measure of effective Pt deposition.[31–33] Fig. S5 shows the stability test results for the catalyst derived from sunscreen-1 for more than 40 h.

The Pt/ZnO catalysts derived from sunscreen-1 and -2 exhibited CO oxidation rates reaching approximately 80% of those observed for catalysts prepared from unmodified ZnO, indicating comparable catalytic performance despite the complex sunscreen matrix. In contrast, the catalyst derived from sunscreen-3 showed almost no detectable CO oxidation activity under the same conditions. Even when the nominal Pt loading was increased to 5 wt% relative to ZnO, no significant catalytic activity was observed.

The scanning transmission electron microscopy (STEM) image and the corresponding energy dispersive X-ray spectroscopy (EDS) elemental mapping images of the Pt/ZnO catalyst derived from sunscreen-1 are shown in Fig. 2(a)–(d). Distinct bright spots attributable to Pt nanoparticles supported on ZnO were clearly observed in the STEM image. In contrast, Si signals, which were attributed to SiO_2 formed by calcination of surface-modified dimethicone, were broadly distributed over the ZnO surface, as revealed by EDS mapping (Fig. 2(c)). However, these SiO_2-derived signals are located at positions different from those of the Pt nanoparticles and are therefore considered to have little to no effect on the catalytic activity for CO oxidation. The Pt nanoparticles exhibited a relatively broad size distribution ranging from 2 to 10 nm, with an average particle diameter of approximately 4 nm (Fig. 2(e)). In comparison, Pt photodeposited on untreated ZnO showed a significantly smaller average particle size of 1.6 nm, with a narrow distribution in the range of 1.0–2.5 nm (Fig. S2). This difference suggests that the existence of surface coating agents on ZnO and additives in the sunscreen matrix influences Pt nucleation and growth.

The XRD patterns of the prepared catalysts are shown in Fig. 3(a) and (b). For all samples, the dominant diffraction peaks correspond to the wurtzite structure of ZnO, and no additional peaks assignable to other metal oxides were detected. For the catalyst derived from unmodified ZnO, no distinct diffraction peak attributable to face-centered cubic (fcc) Pt nanoparticles was observed near $2\theta \approx 40^\circ$, corresponding to the Pt(111) plane. This absence is consistent with the highly dispersed and small Pt nanoparticles observed by TEM. In contrast, a weak diffraction peak near $2\theta \approx 40^\circ$ was detected for the catalyst derived from sunscreen-1, indicating the presence of relatively larger Pt nanoparticles. This observation is in good agreement with the TEM results, which showed a broader particle size distribution and increased average particle size compared to the unmodified ZnO-derived catalyst.

After hydrogen reduction, the catalysts were sealed under an inert atmosphere and subjected to X-ray absorption spectroscopy (XAS) measurements (Fig. 3(c)). The X-ray absorption near-edge structure (XANES) spectra exhibited features characteristic of metallic Pt, confirming the formation of Pt^0 species. X-ray photoelectron spectroscopy (XPS) measurement also confirmed the presence of Pt^0 species and the interaction of Zn and Si (Fig. S4). These results provide direct evidence for the successful deposition of metallic Pt nanoparticles onto ZnO derived from the sunscreen matrix.

When sunscreen products were used as the ZnO source, the organic additives already present in the formulation (*e.g.*, glycols) were expected to function as sacrificial oxidants during the photodeposition process. To evaluate this hypothesis, the catalytic performance of the resulting materials was examined as a function of ethanol addition and irradiation time (Fig. 4). When this validation experiment was conducted using sunscreen-1, comparable CO oxidation rates were obtained even in the absence of added ethanol and with a reduced irradiation time of 4 h. These results indicate that sufficient Pt deposition was achieved under these conditions. However,

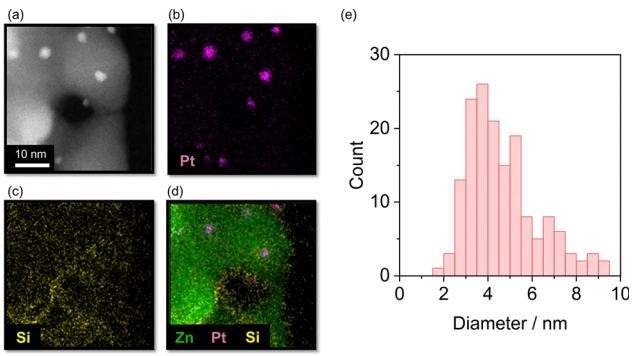

Fig. 2 (a) STEM image; (b) Pt, (c) Si, and (d) overlapped mapping; and (e) Pt particle size distribution of the catalyst derived from sunscreen-1.

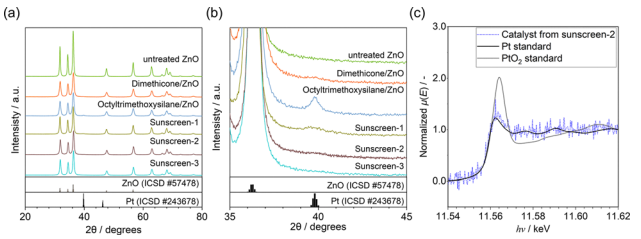

Fig. 3 (a) XRD patterns of Pt deposited ZnO catalysts and (b) their enlarged image. The standard reference data for ZnO and Pt correspond to the wurtzite and face-centered cubic structures, respectively, from the Inorganic Crystal Structure Database (ICSD). (c) *Ex situ* XAS spectrum of Pt deposited ZnO derived from sunscreen-2.

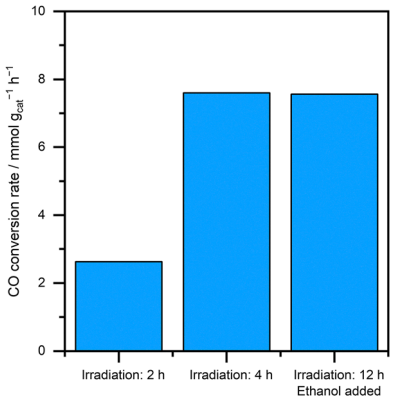

Fig. 4 CO oxidation performance of Pt deposited ZnO catalysts derived from sunscreen-1 with varying UV light irradiation time and ethanol addition. Reaction conditions: catalyst weight = 1.3 mg (diluted with 78.7 mg of Al_2O_3, dilution ratio = 60). Pretreatment conditions: pure H_2, 300 °C, 30 min. Reaction conditions: CO = 0.10 kPa and O_2 = 10 kPa (Ar balance), flow rate = 100 mL min^{-1} (WHSV = 4615 L g^{-1} h^{-1}), 170 °C.

when the irradiation time was further shortened to 2 h, the CO oxidation rate decreased significantly, suggesting incomplete Pt deposition.

In contrast, when unmodified ZnO or dimethicone-coated ZnO was used as the starting material, neither Pt deposition nor subsequent CO oxidation proceeded in the absence of ethanol. These findings demonstrate that, when sunscreen products are used as the ZnO source, the intrinsic organic additives in the formulation can serve as effective sacrificial agents, enabling photodeposition of Pt onto ZnO without the need for additional sacrificial reagents. Because the optimal irradiation time depends on reactor geometry and light intensity, further systematic investigation will be required for practical implementation.

In conclusion, we demonstrated a separation-free chemical upcycling strategy that directly converts disposed sunscreen products into functional Pt/ZnO catalysts by exploiting the intrinsic photocatalytic activity of cosmetic-grade ZnO nanoparticles. Organic components present in the native sunscreen matrix can serve as sacrificial agents, enabling reagent-free photodeposition of metallic Pt without additional reagents. Structural and catalytic analyses revealed that the presence of surface coating agents on ZnO and additives in the sunscreen matrix governs Pt dispersion and accessibility, directly impacting CO oxidation performance. By eliminating conventional purification, solvent exchange, and external reducing steps, this approach provides a practical and materials-efficient route for valorising complex consumer waste streams. In the present study, Pt was employed as a model catalyst to clearly demonstrate the feasibility of our concept. However, this method is not limited to Pt; other more earth-abundant metals (*e.g.*, Ni, Cu or Co) can also be deposited onto ZnO using the same method. This work highlights the potential of transforming complex consumer waste into value-added catalytic materials, offering a practical pathway toward resource circularity.

Conflicts of interest

There are no conflicts to declare.

Data availability

Raw data for each experiment are available by contacting the corresponding author.

The data supporting this article have been included as part of the supplementary information (SI). Supplementary information: experimental details and TG analysis. See DOI: https://doi.org/10.1039/d6cc01514j.

Acknowledgements

This work was based on results obtained from a project, JPNP20004, subsidized by the New Energy and Industrial Technology Development Organization (NEDO). The STEM–EDS mapping measurement was performed at the Advanced Research Infrastructure for Materials and Nanotechnology in Japan (ARIM). The XAS measurements were carried out at the BL14B2 beamline of SPring-8 with the approval of the Japan Synchrotron Radiation Research Institute (JASRI) (Proposal No. 2025B1866). The authors also appreciate the valuable support from the beamline scientists during the XAS experiments.

References

1 H. Chen, K. Wan, Y. Zhang and Y. Wang, *ChemSusChem*, 2021, **14**, 4123–4136.
2 J. M. García, *Chemistry*, 2016, **1**, 813–815.
3 J. Wang, Y. Wang, M. Xiao, Q. Liang, S. Yang, J. Liu, Y. Zhang, H. Mou and H. Sun, *Chem. Eng. J.*, 2024, **484**, 149532.
4 R. Cao, M.-Q. Zhang, C. Hu, D. Xiao, M. Wang and D. Ma, *Nat. Commun.*, 2022, **13**, 4809.
5 Z. Huang, M. Shanmugam, Z. Liu, A. Brookfield, E. L. Bennett, R. Guan, D. E. Vega Herrera, J. A. Lopez-Sanchez, A. G. Slater, E. J. L. McInnes, X. Qi and J. Xiao, *J. Am. Chem. Soc.*, 2022, **144**, 6532–6542.
6 Z. Xu, N. E. Munyaneza, Q. Zhang, M. Sun, C. Posada, P. Venturo, N. A. Rorrer, J. Miscall, B. G. Sumpter and G. Liu, *Science*, 2023, **381**, 666–671.
7 Z. Guo, Y. Li, M. Wang and D. Ma, *Acc. Chem. Res.*, 2025, **58**, 3184–3194.
8 A. M. Martins, A. T. Silva and J. M. Marto, *Sustainability*, 2025, **17**, 5738.
9 K.-B. Kim, Y. W. Kim, S. K. Lim, T. H. Roh, D. Y. Bang, S. M. Choi, D. S. Lim, Y. J. Kim, S.-H. Baek, M.-K. Kim, H.-S. Seo, M.-H. Kim, H. S. Kim, J. Y. Lee, S. Kacew and B.-M. Lee, *J. Toxicol. Environ. Health, Part B*, 2017, **20**, 155–182.
10 M. Verma and K. Pulidindi, *Nano Zinc Oxide Market - by product (coated nano ZnO, Un-coated nano ZnO), by application (personal care & cosmetics, paints & coatings, textiles, electronics) & forecast, 2024-2032*, Global Market Insights Inc., 2024.
11 A. Kołodziejczak-Radzimska and T. Jesionowski, *Materials*, 2014, **7**, 2833–2881.
12 *U.S. Geological Survey, Mineral commodity summaries 2024*, U.S. Geological Survey, Reston, Virginia, 2024.
13 T. Y. Sun, F. Gottschalk, K. Hungerbühler and B. Nowack, *Environ. Pollut.*, 2014, **185**, 69–76.
14 Z. Abbas, S. Zahra, W. S. Shin and S. M. Jung, *J. Environ. Manage.*, 2025, **385**, 125694.
15 S. Luo, J. Liu and Z. Wu, *J. Phys. Chem. C*, 2019, **123**, 11772–11780.
16 R. Sang, Y. Zhang, J. Shao, C. Yan and K. Zhao, *J. Alloys Compd.*, 2019, **777**, 506–513.
17 G. Pacchioni, *ACS Catal.*, 2024, **14**, 2730–2745.

18 M. Behrens, F. Studt, I. Kasatkin, S. Kühl, M. Hävecker, F. Abild-Pedersen, S. Zander, F. Girgsdies, P. Kurr, B.-L. Kniep, M. Tovar, R. W. Fischer, J. K. Nørskov and R. Schlögl, *Science*, 2012, **336**, 893–897.
19 R. Fiorenza, L. Spitaleri, F. Perricelli, G. Nicotra, M. E. Fragalà, S. Scirè and A. Gulino, *J. Photochem. Photobiol., A*, 2023, **434**, 114232.
20 K. Wenderich and G. Mul, *Chem. Rev.*, 2016, **116**, 14587–14619.
21 J. M. De Corrado, J. F. S. Fernando, M. P. Shortell, B. L. J. Poad, S. J. Blanksby and E. R. Waclawik, *ACS Appl. Nano Mater.*, 2019, **2**, 7856–7869.
22 J. F. S. Fernando, M. P. Shortell, C. J. Noble, J. R. Harmer, E. A. Jaatinen and E. R. Waclawik, *ACS Appl. Mater. Interfaces*, 2016, **8**, 14271–14283.
23 S. A. C. Carabineiro, B. F. Machado and G. Dražić.
24 H. S. Gandhi, G. W. Graham and R. W. McCabe, *J. Catal.*, 2003, **216**, 433–442.
25 B. Liu, S. Han, K. Tanaka, H. Shioyama and Q. Xu, *Bull. Chem. Soc. Jpn.*, 2009, **82**, 1052–1054.
26 A. Ghafoor, M. Lotfi, A. A. Gomaa, A. Goldbach and W. Shen, *ACS Appl. Nano Mater.*, 2025, **8**(8), 3887–3898.
27 Y. Song, L. Zhang, Y. Zhang, Y. Wang, Z. Xu and B. Zhang, *Particuology*, 2025, **100**, 36–44.
28 Y. Martynova, B.-H. Liu, M. E. McBriarty, I. M. N. Groot, M. J. Bedzyk, S. Shaikhutdinov and H.-J. Freund, *J. Catal.*, 2013, **301**, 227–232.
29 M. Lotfi, A. A. Gomaa, A. Ghafoor, A. Goldbach and W. Shen, *Appl. Catal., A*, 2025, **699**, 120265.
30 H. Liu, A. Zakhtser, A. Naitabdi, F. Rochet, F. Bournel, C. Salzemann, C. Petit, J.-J. Gallet and W. Jie, *ACS Catal.*, 2019, **9**, 10212–10225.
31 H.-J. Freund, G. Meijer, M. Scheffler, R. Schlögl and M. Wolf, *Angew. Chem., Int. Ed.*, 2011, **50**, 10064–10094.
32 M. A. van Spronsen, J. W. M. Frenken and I. M. N. Groot, *Chem. Soc. Rev.*, 2017, **46**, 4347–4374.
33 A. D. Allian, K. Takanabe, K. L. Fujdala, X. Hao, T. J. Truex, J. Cai, C. Buda, M. Neurock and E. Iglesia, *J. Am. Chem. Soc.*, 2011, **133**, 4498–4517.